Light Metals 2014
Edited by: John Grandfield
TMS (The Minerals, Metals & Materials Society), 2014

Heat Treating of High Pressure Die Cast Components: Challenges and Possibilities

Salem Seifeddine[1,2], Darya Poletaeva[2], Mohammad Ghorbani[2] and Anders Jarfors[2]
[1] Swerea SWECAST, Box 2033, 55002 Jönköping, Sweden
[2]Jönköping University; School of Engineering, Department of Mechanical Engineering, Materials and Manufacturing – Casting, P.O. Box 1026, SE-551 11, Jönköping, Sweden

Keywords: High Pressure Die Casting, Aluminum, EN AC 43100, Solution Treatment, Mechanical Properties.

Abstract

Improving the mechanical properties of high pressure die-cast (HPDC) components through T6 heat treatment is still a challenge due to surface blistering. In the current study, theoretical formulation of porosity growth in cast aluminum, EN AC 43100, has been developed along with differential scanning calorimetry and wave dispersive spectrometry to determine temperature ranges of phase transformations and Al-matrix enrichment of solutes. Optimal combinations of time and temperature for maximum possible Mg dissolution in the Al-matrix without blistering as well as tensile testing on samples extracted from HPDC components and samples from the gradient solidification technique that offers samples with low porosity levels have been performed. The results demonstrate that even if the Mg level in the Al-matrix increases and no blisters on component surface are apparent, the strength outcome is limited and can be degraded. Consequently no guarantees are granted that with a seemingly well performed T6 treatment, strength improvement will be realized.

Introduction

Gas entrapments, in the form of small cavities with sizes of 10-2000 μm, are the most frequent defect found in high pressure die castings. Gas and air bubbles can form in turbulent liquid metal vein or in the shot sleeve, in filling channels or inside die cavity. Also the gases from burning of lubricant which usually consist of hydrocarbons can be entrapped. The porosity morphology appears as spherical or ellipsoidal cavities characterized by relatively smooth surfaces on which a thin oxide layer could be found. The final distribution of cavities within the casting depends on the path of the metal. Due to these gas and/or air entrapment porosity, high pressure die castings are seldom exposed to traditional post solidification treatments and hence, the alloy potential in terms of mechanical properties are hardly realized. Castings based on the Al-Si-Mg system, might attain yield strength levels up to 140 MPa and up to 250 MPa in ultimate tensile strength in as-cast conditions while in the heat treated state, that concerns gravity die and sand castings, the properties could be up to 270 MPa and 300 MPa respectively [1]. The heat treatment cycle is normally the T6-temper that consists of solution treatment, quenching and ageing, either naturally at room temperature or artificially at higher temperature and for faster strength response. Since the solution treatment step is performed to dissolve Mg containing particles, such as the Mg_2Si and the π-Fe phase ($Al_8Mg_3FeSi_6$) formed during solidification and to homogenize alloying elements in the Al-matrix as well as to spheroidize the eutectic Si particles, it is normally conducted at a temperature range 525-540 °C. Quenching is normally done at a high cooling rate to retain a high concentration of vacancies and solute in solid solution and ageing at a lower temperature to form metastable precipitates, that act as hinders for dislocations movements and hence lead to strength increments.

The solution treatment step is normally what limits the application of heat treatment on HPDC components. The reason for this limitation is the large quantity of porosity associated with this casting process that may blister and coalescence, as a result of the solution treatment temperature, due to expansion of the gas trapped inside the pore. These entrapped gases within a sub-surface region can be blown up when the internal pressure of sub-surface gas-related porosity is high enough to plastically deform the thin metallic layer that covers it. The metal deformation occurs also easily at relatively high temperatures, when castings are ejected from the die or during following heat treatments at elevated temperatures. Another consideration is in the swelling, leading to dimensional instabilities resulting in an overall reduction of the mechanical properties [2].

Therefore the challenges lay in applying a solution treatment on HPDC castings that is conducted at low temperature range to prevent surface blistering, yet enough to allow phase dissolution to achieve a certain level of Mg in solid solution for the subsequent ageing process and strength development in the casting. With this in mind, the current paper is aiming at estimating the critical solution treatment temperature for the alloy and the casting produced by the EN AC 43100 alloy in terms of avoiding blistering and increasing level of solutes in the Al-matrix for the subsequent quenching and ageing steps.

Experimental

In order to establish a sustainable manner to predict whether a component with a certain level of porosity is able to be heat treated or not, a theoretical formulation on porosity expansion and hence blistering is developed as a function of temperature. The recommended temperature will be applied during the solution treatment for a variety of time in order to investigate the changes in the level of solutes in the Al-matrix that are available for the subsequent precipitation stage and strength development.

Heating trials on the component

Without any perceptions, a number of components, see figure 1, were subjected to a number of heating trials at temperatures ranging from 450 to 540 °C for a variety of times with the aim to observe when and at what regions blister and/or subsurface coalescence of pores are likely to occur. After the heating operations and mapping of blister formations, all components, including a number of non-heated ones for comparisons of sizes before and after, were subjected to microscopic and porosity investigations in terms of porosity radius, distance to surface, coalescence; valuable data for further estimations of a proper solution treatment temperature without risking surface damages.

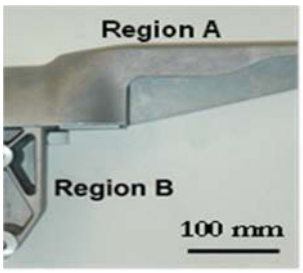

Figure 1. For confidentiality, a part of the component is shown.

Melting – Gradient solidification technique

As a component is exhibiting a wide variation of microstructures and hence properties [3], due to elemental segregations, wall thicknesses, etc. it would not be accurate to extract samples from the casting itself for differential scanning calorimetry (DSC) for phase dissolutions studies. The results will then differ depending on the location and what elements that might be captured at that particular region. Therefore, in order to elucidate the influence of dissolution time and temperature of Mg-bearing phases into the dendrites/Al-matrix and on the resulting mechanical properties of the alloy, excluding the possible effect of the defects associated with HPDC production method, gradient solidified samples were produced [4]. Due to the low level of defects, the samples will also be representing the potential of the alloy in terms of strength.
The gradient solidified samples were produced from the EN AB-43100 ingots that were melted (Al-10.50%Si-0.37%Mg-0.27%Fe using optical emission) into a copper die for production of cylindrical rods with length 180 mm and 10 mm diameter. The rods were remelted and solidified using the gradient solidification technique that also provides a well-fed and homogenous microstructure. By changing the speed of the heating element through the cooling zone in the gradient solidification equipment, different microstructures, defined by the secondary dendrite arm spacing (SDAS) can be produced. In order to select the right cooling conditions, the SDAS and overall microstructure coarseness of the component were examined, based on which a similar microstructure were produced. Figure 2 shows the comparisons of the microstructures by the HPDC process and gradient solidification technique.

It is shown that the average SDAS is of 8-10 µm for both microstructures and the Si morphology is comparable. The only difference that can be seen is the shape of dendrites. It can be assumed to be due to the spray like filling and the friction resistance of primary dendrites during high velocity of injection and in b, is due to directional mode of solidification.

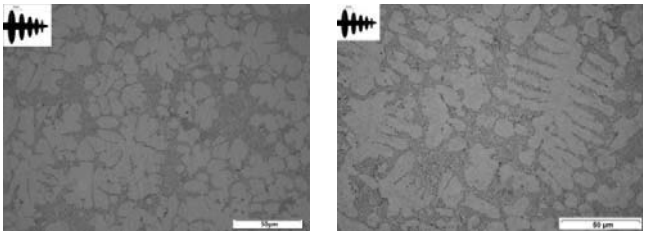
a) b)
Figure 2. a) represents the microstructure of the HPDC component and b) the microstructure by the gradient solidification technique.

DSC and WDS

Thermal analysis was performed using NETZSCH 404C. The specimens for DSC analysis were turned, from the gradient solidified material, to disks of 5 mm diameter and 1 mm height to obtain weight in a range of 40-50 mg. The DSC study was performed in atmosphere of argon using various temperature programs to analyze the possible dissolution sequences. Samples were scanned from 25 to 530°C using heating rates: 2, 5, 10, 15, 20, 25, 30 and 40°C/min and cooling rate of 10°C/min. Wavelength Dispersive Spectroscopy (WDS) was used to measure the concentration profiles of Mg and Si in Al-matrix in as-cast conditions as well as after a variety of solution treatment exposures as a function of temperature and time, then rapidly quenched in 50°C water.

The selection of temperatures is based on the maximum allowed temperature for avoiding blister formations. Samples for the WDS tests were cut from the gradient solidified rods with length approx. 8-10mm. As-cast and solution treated samples at 540°C were used as references for minimum and maximum Mg and Si contents in Al-matrix. Quenched samples were immediately examined or, if this was not possible, were kept in a freezer at the temperature approx. -10°C. Three to five dendrites were measured per sample. Three measurement points were made per dendrite: one point in the center and two others on the sides (2~2.5 μm from the center). The operating voltage 10kV and a beam current of 18 nA were set and pure elements were used as standards to calculate magnesium and silicon content. The width of the beam (diameter of the measurement point) is in the range 1~1.5 μm.

Heat treatment

Various combinations of solution treatment parameters for gradient solidified samples have been carried out. They were based upon concentration measurement results and theoretical calculation of maximum allowable temperatures to avoid porosity expansion. For each heat treatment cycle three samples were used. The countdown of solution treatment time started from minute 15 after inserting samples into the furnace that is preheated to reach solution treatment temperature in the castings. Also a number of samples were subjected to solution treatment at 540°C for 15 minutes, in order to find the maximum strength of the alloy.
All samples were then rapidly quenched in 50°C water. Artificial ageing was conducted in a forced circulation air furnace immediately after quenching. The temperature and time were set standard for all samples: 170°C for 6 hours. Based on the findings, samples from the components are extracted and heat treated for validation purposes.

Mechanical properties

The ASTM B 557M-02a tensile test standard was applied for round samples prepared from gradient solidified rods, as well as for the flat samples extracted from the component, region A, figure 1. The test was performed at a constant strain rate of 0.00025 1/s by using ZWICK/Roell Z100 Tensile Test Machine; preload of 15MPa was applied. The machine was equipped with the clip-on 25 mm gage length extensometer and it was set to fracture of samples.
The high temperatures tensile tests were performed on the same machine according to ASTM E21; the tests were performed at low

strain rate, 0.0001 1/s. Laser extensometer was used to measure the elongation.

Results and discussion

Porosity analysis and theoretical estimation

Subjecting a number of components for a variety of solution treatments indicated clearly the region where the blistering formation frequently appeared. Table 1 clearly reveals the impact of temperature and time on the entrapped gases.

Table 1. Blister size at various temperatures and times

	Temperature(°C)					Blister Size (mm)
Time(min)	450	460	480	500	540	
15					✖	✖ >5
30			X	X		✖ 3-4
60		+	X	✖		X 2-3
120		X	✖			X 0.5-1
180	+					+ <0.5

The results point out that temperatures above 460 °C will readily harm the component. Even the holding time plays a major role. Longer times at those temperatures indicate that creep is taking place; the deformation mechanisms require more investigation and are outside the scope of the current investigation. The majority of blisters were found in region B, figure 1, which is also associated with a large number and sizes of pores, as noticed in figure 3 a. As revealed in figure 3 b, neighboring pores can coalescence due to rupture of cell walls. It was also observed that coalescence occurred far from the surface and together, minor pores formed large porosity without making blisters on the component surface; which might be decisive.

For a blister to occur, the material strength has to be exceeded, and hence there are a number of parameters that are dominant such as the pressure inside the pore, the radius of the pore and its distance to the surface, and temperature and time applied.

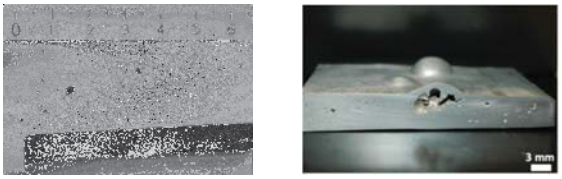

a) b)

Figure 3. Porosity size and distribution in a) as-cast condition, and b) solution treated for 500°C for 60 min.

An approximation of the pore pressure at higher temperature starts by estimating the total pressure of the gas inside the pore at solidification temperatures which is assumed as the multiplication of shrinkage coefficient, eq.1:

$$P_{Total} = \frac{P_{machine}}{1+\beta} \quad (1)$$

The pressure of pore at room temperature follows the Gay-Lussac's Law, eq.2:

$$P_{R.T} = \frac{P_{machine}}{1+\beta} \times \frac{T_{R.T}}{T_{Sol.}} \quad (2)$$

By heating of the component, the pressure of the gas rises, eq.3:

$$P = \frac{P_{machine}}{1+\beta} \times \frac{T}{T_{Sol.}} \quad (3)$$

For estimating the maximum stress, Von-Mises stress formulation of thick-walled vessels under uniform internal pressure generated by heated gas was used [5]:

$$\sigma_{v-Mises} = \frac{3}{2} \times P \times \left(\frac{a^3}{a^3 - b^3} \right) \quad (4)$$

where, P is pressure of the gas inside the pore and b is the radius of pore and a is the distance to surface.(*b/a-b* was assumed as ratio of radius to primary surface distance of porosity). By replacing eq. (3) and (4), the yield strength can be derived for various temperatures versus different radius/thickness (r/t) ratio:

$$\sigma_{V-Mises} = \frac{3}{2} \times \frac{P_{machine}}{1+\beta} \times \frac{T}{T_S} \times \left(\frac{a^3}{a^3 - b^3} \right) \quad (5)$$

Tensile testing at higher temperature was conducted in order to derive the relationship between yield strength and temperature of the current alloy that yields a linear trend as follows in eq.6:

$$\sigma_y(T) = 273.55 - 0.35 \times T \quad (6)$$

By equalizing streses derived by equations (5) and (6), linear relation of temperature versus radius over distance can be derived

$$\frac{3}{2} \times \frac{P_{machine}}{1+\beta} \times \frac{T}{T_S} \times \left(\frac{a^3}{a^3 - b^3} \right) = 273.55 - 0.35 \times T \quad (7)$$

Applied pressure of the HPDC machine on the casting, $P_{machine}$, can be reduced due to changing of cross section in gating system and also different bending angles in runner. For each 90° of bending, 40% of pressure is reduced and each changing in cross section reduces additionally 20% of pressure in liquid phase [6].

According to data provided by producer, the applied pressure were 50MPa including 2 bending of 90° and one changing in cross section at filling gate. The actual applied pressure was 14.4 MPa. With these data available, a relationship between the critical temperature and critical r/t is plotted, assuming high heating rates, see figure 4.

It is apparent that at higher temperatures the critical ratio r/t decreases. Experimental data showed that at 500°C for 60 min, even with a ratio of 0.8 blisters took place. Experimental variations as temperature, visual observations, heating rates, 120°C/min in the current study, where slow rates may cause creep and high rate may influence the transformations and kinetics of phases, time, applied pressure etc. will influence the slope of the curve in figure 4; above the trend line, the risk for blistering is high.

The effect of hydrogen available is estimated to be of a minor importance due to the following calculation; the changes in amount of hydrogen solubility [7] is ΔS_{S-l}=0.343 cm^3/100gr Al.

Since the total pressure in porosity consists of air and precipitation of hydrogen it can be assumed that:

$$P_{Gas} = P_{H_2} + P_{N_2} + P_{O_2} \quad (8)$$

According to Sievert's law, the partial pressure of hydrogen can be calculated considering the effect of surface tension:

$$P_{H_2} = (\frac{S}{K})^2 - \frac{2\gamma}{r} \quad (9)$$

that is 1.2×10^5 Pa. Using general gas law PV=nRT, n = 2.9×10^{-5} moles.

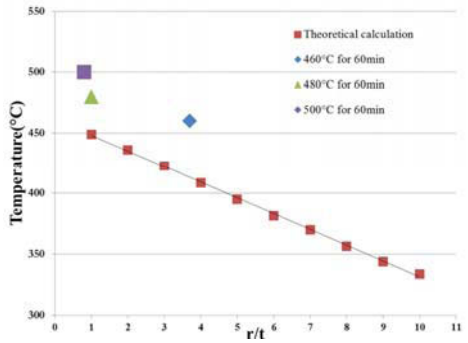

Figure 4. The relationship between solution temperature as a function of r/t; calculated and experimental.

the number of moles that has been entrapped inside the pore was calculated [8]:

$$(moles/m^3) = 1.01\times(cm^3H_2/100gr.Al) \Rightarrow n_{H_2} = 1.33\times10^{-9} Moles$$

Based on large difference between moles of entrapped air and hydrogen, it is concluded that the effect of hydrogen gas in pore pressure evolution is very low.

Exceeding the calculated temperatures resulted in blister formations for similar r/t, figure 4. Based on the theoretical estimation with measured critical r/t from as-cast components and blister formation investigation, it was found that solution treatment of this component might be performed in the range of 460-480 °C; a step higher than the estimated ones. In order to optimize the solution treatment temperature and time, the level of solutes in solid solution at solution treatments for optimized mechanical performance has to be identified, why DSC and WDS analysis are carried out.

Differential scanning calorimetry and concentration profiles

The result of thermal analysis is 8 DSC curves corresponded to 8 different scanning rates, figure 5. It can be observed that with increasing scanning rate the starting temperature for transformation of various phases (precipitation sequence) increases proportionally. Reaction with low heat content cannot be detected with low scanning rate. It is happening due to slow transition between phases and gradual relaxation of energy corresponded to those transitions. Due to absence of reference material during the analysis, obtained DSC curves with high scanning rates have a parabolic behavior and starting temperature of the first monitored reaction is 233.3°C.
The first observed exothermic peak with maximum at 283°C in a temperature range 230-350°C can be a transformation of available Mg:Si metastable phases, β'' or β', and might also be linked to the fact that Si is diffusing to pre-existing eutectic Si particles.

But due to possible overlapping of two or more reaction peaks it does not seem possible to define amount of relaxed energy individually. The metastable phases form, as Si and Mg in solid solution are available, in the Al-matrix during solidification, but at low levels. Dutta et al. [9] has also monitored a very wide peak that firstly was related to β'' formation, but after a series of experiments it was assumed that it was a merging or overlapping of two peaks corresponded to formation of β'' and β' phases at 232°C and 242°C respectively.

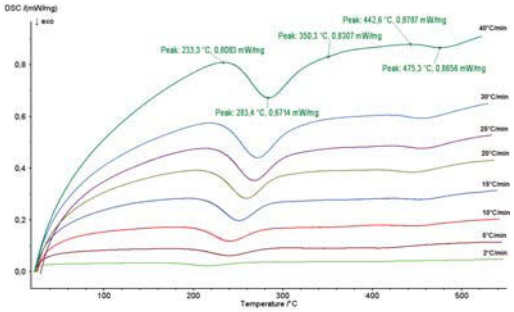

Figure 5. DSC for as-cast samples at different scanning rates.

TEM analysis of the alloy samples heated to those temperatures revealed the microstructure consisting mostly of dot-like and needle-like precipitates at first peak and needle-shaped precipitates with easily defined size at second peak [9]. Incoherent equilibrium Mg_2Si β-phase, forms in the second exothermic peak (440-520°C) with maximum at approximately 475°C as observed in figure 5. At this range, the π-Fe is also likely to break up releasing Mg into solid solution. Due to end temperature of the scan, 530°C, the start temperature of dissolution reaction of Mg_2Si phase was not detected. However, peaks with similar temperature ranges were obtained in other research [9], which also includes endothermic dissolution reaction started at 522°C with maximum at 547°C.

In the microstructure, figures 2, the Mg_2Si is though hardly presented compared to π-Fe that is also in accordance with Sjölander [10], which is also a function of SDAS, as reported. Therefore, it is assumed that the latter one is the main contributor to the Mg diffused into solid solution during the solution treatment while itself it is transformed into Al_5FeSi plates. Literature shows that dissolution of the Mg_2Si phase in the Al-7%Si-0.4%Mg alloy was completed after 2–4 min and homogenization was completed after 8–15 min. But, the more Mg in the alloy and the larger SDAS, the dissolution and homogenization processes take longer times [11-13]. If the Mg concentration is low (0.3–0.4 wt%), which is the matter in the current study, the transformation is fast [14-15].

Unfortunately, DSC instrument does not detect phase reactions during isothermal holding at constant temperature. And it was impossible to predict exact time of full dissolution of Mg-bearing phases at low temperature solution treatment using this technique. Thus, WDS analysis was used to further investigate concentration profiles of Mg and Si after solution treatment at 460 and 480 ^{0}C. Trends from the WDS analysis are presented in figure 6, but no absolute values, which requires other instruments. As depicted, in as-cast conditions the Mg content is around 0.04wt% which is about 11% of the Mg level in the alloy (0.37wt%). Solution treated at 540°C, the Mg level was remarkably increased. Average Mg content was 0.32wt% which is 86% of total amount of Mg, which is in agreement with Rometsch and Arnberg [11].
The level of Si in Al-matrix after solution treatment at 540^{0}C for 15 min decreased till 1.20 wt% from 1.51 wt%, closer to equilibrium level 1.06 wt%, figure 6.

As witnessed in figure 7a, with increasing time of the solution treatment at 460^{0}C the amount of Mg in Al-matrix increases. After 2 hours at 460^{0}C, almost full dissolution of Mg-bearing phases can be achieved. After solutionizing at 460°C for 15

minutes the level of Si decreases to the range 0.71-0.77 wt% and it is close to equilibrium level, 0.6-0.65 wt%, figure 7b.

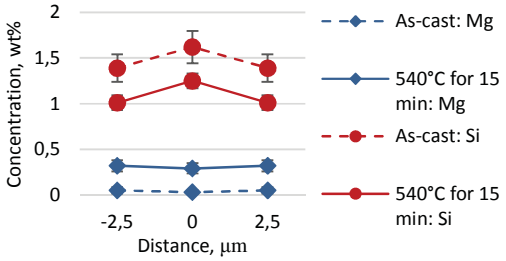

Figure 6. The distribution of Mg and Si across the Al-dendrite in as-cast condition and after 15 min of solution treatment at 540°C.

Dons et al confirmed, with simulation, that similar anomalous concentration profiles were developed only in the samples with high cooling rate and caused by back diffusion of Si outside of the Al-matrix to eutectic Si particles [16].

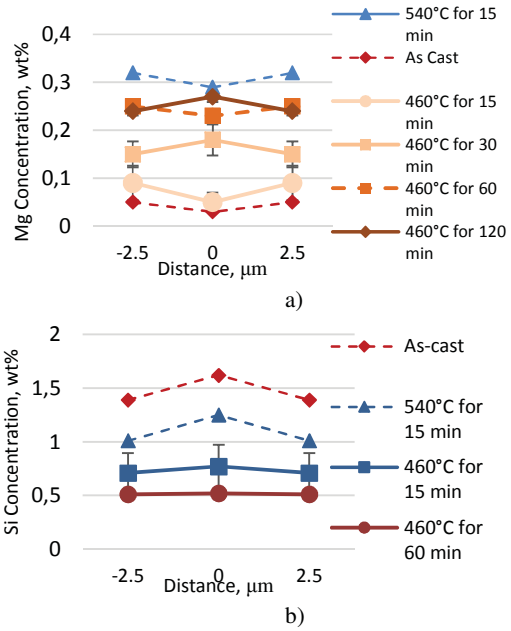

Figure 7. a) Mg and b) Si levels in Al-matrix (dendrite).

It is also detected that after 1 hour of solution treatment there is a drop in level of Si from 0.77 wt% to 0.52 wt%. However, visual examination of the microstructure did not indicate any significant changes in the eutectic Si morphology. Robinson [17] obtained similar results during interrupted quenching experiment at 450°C where any quench precipitates was not observed; instead, a drop in hardness was detected, explained by loss of Si in solid solution.

After 30 minutes at 460° and 480°C the concentration of Mg in Al-matrix was almost at the same level, 0.17 wt% with a difference only of 0.01 wt%. The Mg level continued to increase after 60 min, but without any significant difference between concentrations at both temperatures. Concerning the Si concentration, a drop was observed after 15 minutes of solution treatment at 460°C, which can be explained by the tendency of the alloy to reach equilibrium level. However, the Si concentration in the dendrite at 460°C continued to decrease down to levels of 0.53 wt%, due to possible back diffusion. Solution treatment at 480°C for 1h, was not enough to reach equilibrium level of Si (0.78-0.8 wt%), the Si level was nearly1 wt%.

With this in mind, few solution treatment temperature programs have been derived, see x-axis in figure 8, for further heat treatment and mechanical testing of gradient solidified samples before using the samples extracted from components for validation in terms of both blistering and strength. Also approximate amount of hardening precipitates were calculated assuming that Mg:Si ratio is close to 1.73 [18].

Mechanical properties

The alloy performance is directly linked to process parameters, component design as well as to local solidification and post solidification treatments. In the current study, the potential of the alloy is presented in figure 8 in as-cast conditions, left bars in the figure, as well as in a heat treated state at 540°C, bars on the right side. Depending on the post solidification treatment and its parameters in terms of temperature and time in the solution treatment stage, a wide variety of properties might be developed as observed in figure 8.

Higher temperature of solution treatment and prolonged time contributed to better 0.2% proof stress, Rp 0.2%, performance, which is an agreement with the trends confirmed by WDS analysis. However, the ultimate tensile strength, Rm, of the as-cast sample is higher than the majority of the proposed treatments. As revealed from the WDS analysis a reduction of Si level in the Al-matrix is detected. For instance, the amount of Si is three times higher in the dendrite in as-cast condition than after solution treatment at 460°C for 60 min. The amount of Mg in Al-matrix after solution treatment at 460°C for 120 min and 480°C for 30 min detected in center of dendrite is 0.26 wt% and 0.17 wt% respectively. But worth to note is that difference in Si levels, 0.53 wt% compared to 1.2 wt%. If only focusing on Mg dissolution it might be concluded that Rp 0.2% of sample treated at 460°C for 120 min will be higher compared to 480°C for 30 min.

But, the fact points out an obvious degradation in mechanical performance for mentioned temperature programs as the average Rp 0.2% drops from 208MPa to 158MPa, Rm from 269MPa to 225MPa respectively. Initially it was assumed that amount of Si in Al-matrix after solution treatment at 460°C for 120 min was not enough to form hardening precipitates and contribute to mechanical performance of the alloy. According to Maruyama et al [19] Mg:Si ratio is increasing through the phase transformation, but it is always ≥ 1, which in this study was fulfilled. This means there is no apparent evidence of excess Mg in the Al-matrix. Gupta et al [18] concluded instead that excess Si > 0.9 wt% increases the effective amount of hardening precipitates.

Therefore, it was decided to subject component samples to solution treatment at 460°C for 1 hour, quenching in 50°C water and ageing at 170°C for 6 hours. The mechanical performance of the components is presented in figure 9. Even though a part of the Mg-bearing phases where broken up and Mg atoms were enriching the Al-matrix, as all WDS results on the samples evident, the departure of Si form the matrix to existing Si particles (from 1.62% down to 0.52%) in the eutectic is seemingly more impacting in realizing a strength increment; thus, the mechanical properties did not improve. As the fracture surfaces of the component samples envisage, large number of porosity as well as

slight tendency towards blistering could be other reasons for premature failures, see figure 10.

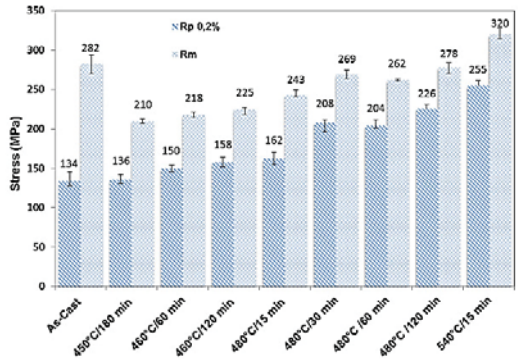

Figure 8. Illustration of the variation of mechanical properties as a function of solution treatment temperatures and times.

Moreover pre-solidified droplets, see encircled regions, due to violent and turbulent filling when fine drops of the cast alloy get into contact with the mold and rapidly solidify. Even though heating trials and naked eye could suggest 460 °C, it seems that the calculated temperature has been more favorable to apply. But, since the dissolution process at lower temperatures would be more energy and time consuming, the industry will not find it appropriate and legitimate. Therefore, if heat treatment of HPDC components is to be useful and the strength potential and the possibility to offer high strength components in cast aluminum to be realized, as depicted in figure 8, vacuum systems in the HPDC machine are to be employed as to control the air entrapment.

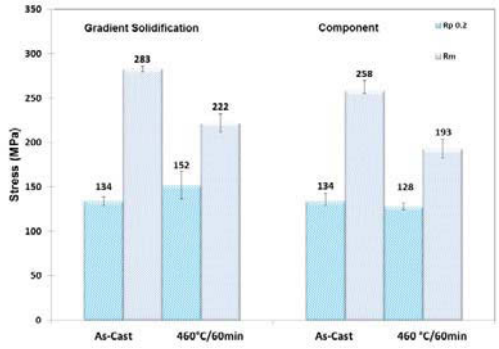

Figure 9. The mechanical properties of gradient solidified and component samples in as-cast and heat treated conditions.

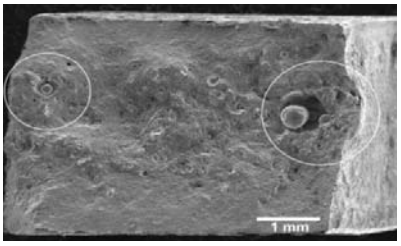

Figure 10. Fracture surface of a component sample exposed to the optimized solution treatment cycle.

Conclusions

The main conclusions are:

1. Depending on porosity size and its distance to surface, a proper solution treatment temperature is selected.
2. Mg-bearing phases are dissolved at relatively low solution treatment temperature but a longer time is required to homogenize the concentration.
3. At low solution treatments, Si atoms are migrating from the matrix towards existing Si in the eutectic, confirmed by WDS.
4. It is not enough to increase the Mg concentration and maintain a ratio with the level of Si; to reach closer to the potential in terms of strength, the level of defects must be kept low.

Acknowledgement

The funding agency Vinnova is acknowledged for partially funding the research activities.

References

[1] Rometsch, P.A. and Schaffer, G.B.," Quench modelling of Al–7Si–Mg casting alloys", *Int. J. Cast Metal. Res*., 2000, 12, 431-439.
[2] Bonollo F., *New quality and design standards for aluminium alloys cast,* 2012.
[3] Seifeddine S. and Svensson I.L., "Prediction of mechanical properties of cast aluminium components at various iron contents" *Materials & Design* 2010, 31, S6-S12.
[4] Seifeddine S., "Characteristics of cast aluminium-silicon alloys: microstructures and mechanical properties" (Ph.D. thesis, Linköping University, 2006).
[5] Young ,W. and Budyans.R., *Roark's formulas for stress and strain*, 7Th Edition, 2002.
[6] ASM Handbook, Castings, Gating Design, 15, 1993, 1280.
[7] Fredriksson, H. and Åkerlind, U., *Materials processing during casting*, 2006.
[8] Anson, J.P., "The nucleation and growth of Microporosity in Aluminum - 7% Silicon Foundry Alloy", (Ph.D. thesis, University of Queensland, 2000).
[9] Dutta, I. and Allen, S.M. "A calorimetric study of precipitation in commercial aluminium alloy 6061", *Journal of Materials Science Letters*, 1991, 10, 323-326.
[10] Sjölander E., "Heat treatment of Al-Si-Cu-Mg casting alloys" (Ph.D. thesis, Chalmers University of Technology, 2011).
[11] Rometsch, P.A., Arnberg, L. and Zhang, D.L.,"Modelling dissolution of Mg2Si and homogenisation in Al–Si–Mg casting alloys", *Int. J. Cast Metal. Res.*1999, 12, 1–8.
[12] Closset, B., Drew, R.A.L. and Gruzleski, J.E., "Eutectic silicon shape control by in situ measurement of resistivity". *AFS Trans* 1986, 94, 9–16.
[13] Shivkumar S., et al.,"Effect of solution treatment parameters on tensile properties of cast aluminum alloys". *J. Heat Treating* 1990, 8, 63-70.
[14] Dons, A.L. and Pedersen, L., Brusethaug, S., "Modelling the microstructure of heat treated AlSi foundry alloys" *Aluminium 2000*, 76, 294–297.
[15] Taylor, J.A. et al.," Influence of Mg content on the microstructure and solid solution chemistry of Al–7%Si–Mg casting alloys during solution treatment", *Mater. Sci. Forum* 2000, 331-337, 277–282.
[16] Dons, A.L., Pedersen, L. and Arnberg, L, "The origin of 'anomalous' microsegregation in Al-Si foundry alloys - modelling and experimental verification", *Material Science A*, 1999, 271, 1-2, 91-94.
[17] Robinson, M. (Thesis, University of Queensland, Australia, 1996).
[18] Gupta, A.K., Lloyd, D.J. and Court, S.A, "Precipitation hardening in Al-Mg-Si alloys with and without excess Si" *Materials Science and Engineering A*, 2001, 316, 11-17.
[19] Maruyama, N. et al., "Effect of silicon addition on the composition and structure of fine-scale precipitates in Al-Mg-Si alloys" *Scripta Materialia*, 1997, 36: 89-93.